Journal Pre-proof

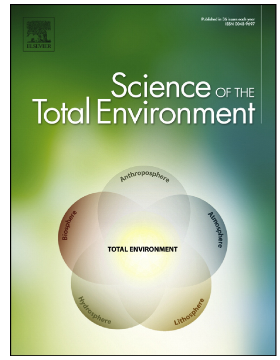

Global and local sensitivity analysis to improve the understanding of physically-based urban wash-off models from high-resolution laboratory experiments

J. Naves, J. Rieckermann, L. Cea, J. Puertas, J. Anta

PII: S0048-9697(19)36148-0

DOI: https://doi.org/10.1016/j.scitotenv.2019.136152

Reference: STOTEN 136152

To appear in: *Science of the Total Environment*

Received date: 24 October 2019

Revised date: 28 November 2019

Accepted date: 14 December 2019

Please cite this article as: J. Naves, J. Rieckermann, L. Cea, et al., Global and local sensitivity analysis to improve the understanding of physically-based urban wash-off models from high-resolution laboratory experiments, *Science of the Total Environment* (2019), https://doi.org/10.1016/j.scitotenv.2019.136152

Global and local sensitivity analysis to improve the understanding of physically-based urban wash-off models from high-resolution laboratory experiments

Naves[1,*], J., Rieckermann[2], J., Cea[1], L., Puertas[1], J. and Anta[1], J.

[1]. Universidade da Coruña, Water and Environmental Engineering Research Team (GEAMA), Civil Engineering School, Elviña, 15071, A Coruña, Spain

[2]. Eawag, Swiss Federal Institute of Aquatic Science and Technology, CH-8600, Dübendorf, Switzerland

*. Corresponding author

e-mail address: juan.naves@udc.es (Juan Naves)

ABSTRACT

Physically-based urban wash-off models are a promising means of studying the transport of finer suspended solids and their associated pollutants during rain events, considering spatial and temporal heterogeneities. This study contributes to the understanding of these models through an in-depth sensitivity analysis to provide the necessary information to simplify the model and deal with parameter identifiability. First, based on twelve tailored high-resolution experiments, the accurate measurement of input variables was used to study the parameters of the Hairsine-Rose sediment transport model through a global sensitivity analysis. Using Standardized Regression Coefficients (SRC) and Extended Fourier Amplitude Sensitivity Test (EFAST) methods, the analysis showed that both the total washed-off mass and the TSS peaks concentration are highly sensitive to the critical mass, which considers the reduction in the detachment of particles when the sediment available decreases and is scattered over the surface. In addition, the rain- and flow-driven detachment parameters were presented as key for smaller and larger sediment particles, respectively. Then, those uncertainties that are associated in field studies with the determination of the model input variables were also considered by conducting a local sensitivity analysis. The initial load of sediment and the mean grain size were seen to be the most important variables, thus underlining the need for very accurate measurements here. Moreover, a precise definition of Harsine-Rose parameters is also necessary to achieve reliable results in order to work on treatment and management techniques to minimize the impact of urban surface contaminants on urban environments.

KEYWORDS:

Urban wash-off modelling

Hairsine-Rose model

IBER

2D shallow water model

Sensitivity analysis

1. INTRODUCTION

The trend towards rapid urbanization and population migration to towns and cities has led to the development of more impervious surfaces, which themselves become a major contributor of pollutants in urban areas (Butler and Davies 2010). Urban runoff contains dissolved and suspended solids that have accumulated in streets, roofs and other surfaces, and are washed-off during rain events (Zafra et al. 2008). Heavy metals and Polycyclic Aromatic Hydrocarbons (PAH) are traditionally considered to be the major causes of contamination in urban stormwater and have been found to be associated with fine particles (Herngren et al. 2005, Akan and Houghtalen 2003, Sartor and Boyd 1972). In addition, recent studies (Dris et al. 2015, Dehghani et al. 2017, Vogelsang et al. 2019) have highlighted the significant presence of microplastics (sizes from 0.1 to 1000 μm) in urban catchments. Thus, the transport process of these fine particles can be used to study stormwater quality during rain events, typically using the concentration of total suspended solids (TSS) as indicator (Rossi et al. 2009, Sikorska et al. 2015).

A thorough understanding of the processes involved in the wash-off of suspended solids, then, is essential in estimating runoff pollution loads and concentrations, and in improving treatment and management techniques to minimize their impact on the environment (Anta et al. 2006). To that end, empirical wash-off equations (e.g. Sartor and Boyd 1972, Egodawatta et al. 2007, Leutnant et al. 2018, Muthusamy et al. 2018) have been developed and implemented in urban drainage models like SWMM (Rossman, 2015) over the last 40 years, but without significant advances in prediction accuracy (Schellart et al. 2010, Gorgoglione *et al.* 2019)). These lumped formulations take as the main variables the initially available sediment load or the total runoff volume, and neglect spatial heterogeneities (Wang et al. 2011), which has the effect of only roughly approximating the complexity of the physical phenomena. Specifically, they do not take into account processes such as the detachment of soil particles due to raindrop impacts or runoff shear, the transport of these particles by the overland flow, or their deposition. Hence, the predictive results obtained are rather uncertain, and they are not particularly useful for engineering risk assessment or design.

Given these limitations of empirical lumped equations to adequately model a complex process such as urban wash-off, several physically-based models have arisen as alternatives. Deletic et al. (1997) considered the spatial distribution of solid particles over the street surface and developed a new formulation, including the rainfall and the shear stress of the overland flow as main variables, to model the entrainment of the particles into suspension. In the wash-off model proposed in Shaw et al. (2006, 2009), the particles are suspended due to raindrop impacts on the flow, in which they are transported until their deposition. In the model introduced by Massoudieh et al. (2008), this particle detachment was assumed to be a function of flow velocity. All these studies showed the potential for modelling the wash-off processes in impervious surfaces with physically-based formulations, but their 1D approximation limits their performance in real urban catchments. More recently, Hong et al. (2016a, b, 2019) evaluated and calibrated the urban wash-off process on a road catchment of 2661 m^2 using the physically-based Hairsine-Rose (H-R) formulation (Hairsine and Rose, 1992a, b) coupled with a 2D shallow water model. Their results showed a promising level of agreement with respect to the field-measured pollutographs, suggesting that 2D physically-based wash-off models could be a feasible alternative to empirical wash-off equations for a better representation of the spatial and temporal heterogeneities in urban water quality studies.

However, several difficulties remain in the use of physical-based models to simulate urban wash-off: i) the high computational cost of these models currently limits their application to small urban catchments; ii) the H-R model was originally developed for, and is usually applied to, model erosion in rural catchments (Cea et al. 2016, Heng et al. 2011), so the lack of experience in urban catchments and the large number of variables needed to model the physical processes render the calibration of the model difficult; iii) due to the randomness and variability in the build-up process (Wijesiri et al. 2015a, Sandoval et al. 2018), uncertainty measuring some input variables, such as the initial load and the sediment distribution over the street surface and characteristics, can lead to unreliable model results in real-world studies.

Therefore, the aim of the present study is to contribute to the understanding of physically-based wash-off models in urban catchments by means of a rigorous sensitivity analysis, this on the basis of a series of specifically designed full-scale laboratory experiments. In these, the physical properties, initial mass and spatial distribution of the deposited sediments in the surface were accurately measured under controlled laboratory conditions. This has allowed the assessment of the model sensitivity to the H-R model parameters through a global sensitivity analysis. Then, the uncertainties associated to all model inputs were considered in a local analysis to assess the relative importance in the water quality results of hydraulics, sediment inputs, and H-R model parameters. Hence, this study is novel regarding three specific aspects:

- The Hairsine-Rose wash-off model was applied coupled with a 2D shallow water model that was previously calibrated with experimental surface velocity and flow data to have the most realistic description of rainfall-runoff transformation.
- A series of tailored wash-off experiments were performed, where the wash-off process was accurately monitored under laboratory-controlled conditions. This experimental data is unique because they were obtained on a 1:1 scale including a realistic rainfall simulator of 36 m^2, using three rainfall intensities and four realistic sediment distributions with different uniform grain sizes. In addition, the data is openly available, which makes our research reproducible and enables others to test their own models and hypotheses.
- The results from our global and local sensitivity analyses provide the necessary information to choose the most important parameters and simplify the model to

make it feasible to transfer the Hairsine-Rose erosion model to a broad field of scientific studies and practical applications in urban catchments.

The remainder of the paper is structured as follows: the numerical model, the laboratory experiments, and the global and local sensitivity analysis methodology are described in Section 2; the results of the sensitivity analyses are set out in Section 3; Section 4 offers a discussion of the results; and finally, general conclusions of the study are presented in Section 5.

2. MATERIALS AND METHODS

The physically-based wash-off model and the different variables and parameters involved are introduced first, in Section 2.1. Then, Section 2.2 includes a description of the experimental facility and the methodology used in the laboratory experiments, which are used as a basis for the sensitivity analysis (SA). Section 2.3 and 2.4 describe the procedure and methods used to perform the global and the local SA. Finally, the ranges of the input factors considered, the implementation of the SA methods, and a preliminary assessment of model predictions, are set out in Sections 2.5, 2.6 and 2.7, respectively.

2.1. Numerical model

The physically-based urban wash-off model used in this study consists of a process-based H-R formulation coupled to a 2D shallow water model. The model was previously applied to soil erosion modelling in Cea et al. (2016). The only modification required for its application to urban environments was the definition of a non-erodible layer corresponding to the impervious surface.

2.1.1. Hydrodynamics

The model Iber (Bladé et al. 2014; García-Feal et al. 2018) was used as a basis for the implementation of the Hairsine-Rose sediment transport equations. This hydrodynamic model solves 2D unsteady depth-averaged shallow water equations using an explicit unstructured finite volume solver, including rainfall and infiltration terms in the mass conservation equation, and using the Manning formula to compute bed friction. Previous studies have shown the capacity of the model to adequately represent the spatial distributions of water depth and velocity under overland flow conditions and including rainfall-runoff transformation (Cea et al., 2010, Cea and Bladé 2015). The runoff model has also been validated for urban areas in the same laboratory facility described in this work (Fraga et al. 2015, Naves et al. 2019b) and also in field applications (Fraga et al. 2016). The input factors in the hydrodynamic equations are the rain intensity (R), the bed roughness Manning coefficient (n), and the surface initial losses (IL).

2.1.2. Wash-off model

The original H-R model uses a vertical layer structure where the sediments can be part of three different compartments. The first compartment is the original soil from which sediments can be detached through the effect of raindrop impacts or through the shear generated by overland flow. The eroded sediments become part of the flow's suspended solid concentration, and can remain in the flow or be deposited over the bed, forming a deposited layer from where they can become re-detached. In the application of the formulation to urban drainage, the original soil corresponds with the impervious surface, so the interactions with the flow are only made from the deposited layer, which is where the urban surface sediments build up. In this way, the time (t) and spatial (x, y) evolution of the suspended sediment concentration is computed by partial derivates from the following depth-averaged equation:

$$\frac{\partial hC}{\partial t} + \frac{\partial q_x C}{\partial x} + \frac{\partial q_y C}{\partial y} = e_r + r_r - d$$

(1)

where C (kg/m^3) represents the depth-averaged concentration of sediment in the water column, h (m) is the water depth, q_x and q_y (m^2/s) are the two components of the specific discharge, e_r (Kg/m^2/s) and r_r (Kg/m^2/s) are, respectively, the rainfall-driven and flow-driven detachment rates from the deposited layer, and d (Kg/m^2/s) is the deposition rate.

The rainfall-driven detachment rate e_r is usually assumed to have a linear relation with rain intensity (Sharma et al., 1993, 1995; Gao et al., 2003) and is computed as:

$$e_r = \alpha R \varepsilon$$

(2)

$$\varepsilon = min\left[\frac{Ms}{Ms_{cr}}, 1\right]$$

(3)

$$\alpha = \begin{cases} \alpha_0, & h \leq h_0 \\ \alpha_0 \left(\frac{h_o}{h}\right)^b, & h > h_0 \end{cases}$$

(4)

where α_0 (kg/m^2/m) is the rainfall detachability coefficient, h_o (m) is a water depth threshold from where the rainfall detachment rate begins to decrease due to the damping of the rainfall energy on the water layer, b is a constant exponent, ε is a correction coefficient to account for the availability of sediment over the impervious non-erodable surface, Ms (Kg/m^2) is the mass of deposited sediment per unit surface, and Ms_{cr} (Kg/m^2) is the mass of sediment over the non-erodable layer needed to achieve the potential rain-driven detachment. Some authors do not implement the correction coefficient ε when modelling soil erosion in rural catchments because in such applications the availability of deposited sediment is guaranteed. This is not the case in urban environments, where the small amount of sediment available over the impervious layer, as well as its heterogeneous distribution, makes it necessary to include this parameter in the model. In this way, it is possible to consider the lower detachment rates in areas where the mass of deposited sediments is low, as well as the decrease in the detachment rate produced when the sediment is being washed-off.

The flow-driven term r_r models the transfer of solids due to the effect of bed friction and is computed using the following equation:

$$r_r = \begin{cases} \frac{\rho_s F(\Omega-\Omega_0)\varepsilon}{(\rho_s-\rho_w)gh}, & if\ \Omega > \Omega_0 \\ 0, & otherwise \end{cases}$$

(5)

where ρ_s and ρ_w (kg/m^3) are the density of the solid particles and water, respectively, Ω (W/m^2) is the runoff stream power per unit surface, Ω_0 (W/m^2) is the critical stream power threshold below which the entrainment rate is zero, F is the fraction of stream power excess over Ω_0 that contributes to the entrainment of sediments, g (m/s^2) is the gravity acceleration, and ε is a correction coefficient to account for the availability of deposited sediment, as explained above. This formulation assumes that only a fraction of the total stream power dissipation, given by $F(\Omega - \Omega_0)\varepsilon$, contributes to sediment detachment and the rest is spent in other head losses.

The deposition rate d of solids from the flow to the surface is modelled as:

$$d = \rho_s w_s C$$

(6)

where w_s is the settling velocity of sediment particles (m/s), which depends on the density and the mean diameter (D_{50}) of the particles, and is computed using the formulation of Van Rijn (1984).

Finally, the evolution of the sediment mass in the surface is computed by solving the following mass balance equation:

$$\frac{\partial Ms}{\partial t} = d - (e_r + r_r)$$

(7)

2.2. Laboratory experiments

A series of wash-off experiments performed in an urban drainage physical model have been used as the basis for a SA of the wash-off model. The advantage of using these experiments instead of field data is that the variables involved in the wash-off process can be measured with a high degree of accuracy under controlled laboratory conditions. In our case, the initial sediment conditions and the rest of hydraulic input factors could be fixed to a constant value, and the global SA was focused on the influence of the poorly-known H-R parameters. The experiments were also used to determine the ranges of the local SA, where hydrodynamic variables and parameters, and initial sediment conditions, are considered.

The experimental facility is located in the Hydraulic Laboratory of the CITEEC, at the University of A Coruña, and consists of a 36 m^2 full-scale street section. A rainfall simulator is located 2.6 m over a concrete street surface, which is divided into a sidewalk and a roadway (Figure 1). The detailed surface elevation data of the facility and the details of the rainfall simulator, which is able to generate rain intensities of 30 mm/h, 50 mm/h and 80 mm/h with high spatial uniformity, were described in Naves et al. (2019b). The generated rainfall-runoff drains into two gully pots located along the curb and into a lateral outflow channel. The surface has an approximate transversal slope of 2% up to the sidewalk and a 0.5% longitudinal slope up to the outflow channel.

The experiments consist of measuring the hydraulics and the total suspended solids (TSS) at the entrance of the gully pots, given a known initial load of sediment over the roadway surface. The initial amount and spatial distribution of sediments over the surface have been determined following previous wash-off studies by the authors (Naves et al. 2017) and the references included therein. The initial load of sediment was fixed to 20 g per meter of curb. It was distributed realistically over the street section, following the results of Sartor and Boyd (1972), since it is known that roadway sediments tend to accumulate close to curbs (Grottker 1987; Deletic and Orr 2005). As shown in Figure 1, most of the sediment (78%) was placed homogeneously within the first 0.15 m from the curb. 10% and 9% of the sediment was then placed over the next 0.15 and 0.70 m, and the remaining 3% over the rest of the surface up to the road median, which in our case was fixed at 2 m from the sidewalk. The sediment deployed was collected from a real road surface, which is described in Fraga et al. (2016), and sieved to obtain four different uniform granulometries (sediment classes in Table 1) with gradation coefficients ($\sigma_g = \sqrt{D_{84}/D_{16}}$) between 1.3 and 2.2 (Julien 2010). The density of the material, measured by a pycnometer for all the granulometries, was 2557±16 kg/m^3, this corresponding to a high value within the range obtained in Pitt et al. (2004), where different urban build-up studies were reviewed.

Each laboratory experiment involves the combination of a sediment class (D1-D4 in Table 1) with steady, homogeneous rainfall of 30, 50 or 80 mm/h intensity, with a duration of 5 minutes. The water discharge through both gully pots was measured by means of a triangular weir and an ultrasonic distance sensor (UB500-18GM75-I-V15, Pepperl and Fuchs), while the TSS were obtained from 200 mL manual grab samples taken at regular time intervals. At the end of the experiment, the solids that remained in the physical model were collected to verify the correct operation of the experiments through a sediment mass balance. The mass balance errors remained below roughly the 5% of the total mass, which is very satisfactory considering the complexity of the physical phenomena. The detailed methodology to perform the mass balance can be found in Naves et al. (2017). The plots in Figure 2 show the flow and TSS results for rain intensities of 80, 50 and 30 mm/h and for the different grain sizes. In addition, a more detailed description of the physical model and those experimental results not included here have been uploaded to the open-access repository Zenodo (Naves et al. 2019a). The hydraulics of the experiments has already been calibrated successfully, using the measured hydrographs with the 2D shallow water model in Naves et al. (2019b).

2.3. Global sensitivity analysis

A global SA (Saltelli et al. 2008) was performed to investigate the variability of the model output under changes in the H-R model parameters. The SA methods and metrics were constrained by the high computational time of the model and the high number of input factors. Thus, to make analysis feasible, the rest of the input factors were not considered, their values being fixed according to the initial conditions of each laboratory experiment. Global SA was evaluated using two techniques: the Standardized Regression Coefficients (SRC), obtained from a multiple linear regression; and the Extended Fourier Amplitude Sensitivity Test (EFAST), which is able to consider the effect of the interactions of factors. These two methods have been applied recently in the field of urban drainage in Gamerith et al (2013) and Donckels et al. (2014), respectively. In addition, Vanrolleghem et al. (2015) and Mannina et al. (2016) used both methods at the same time, showing that robustness of global SA is substantially increased by using multiple methods and multiple objectives.

2.3.1. *Standardized Regression Coefficients (SRC)*

Standardized Regression Coefficients (Helton, 1993) were used as quantitative measures of the sensitivity of the model outputs to the H-R parameters considered (Saltelli et al. 2000, Saltelli et al. 2008). The multiple linear regression model takes the following form:

$$y_i = b_0 + \sum_{j=1}^{n} b_{ij} x_{ij} + \xi \quad (8)$$

where y_i are the different outputs studied, x_i $(x_{i1}, x_{i2}, \ldots, x_{in})$ are the n parameters vectors, b_j are the regression coefficients, and ξ is the residual error due to the linear approximation. The SRC (b_stand_{ij}) measure the effect of the input factors (x_j) in the variance of the output (y_i), and are obtained as:

$$b\_stand_{ij} = b_{ij}\sqrt{\frac{Var(x_{ij})}{Var(y_i)}}$$

(9)

The absolute value of the regression coefficients represents the influence of each parameter to a certain model output, with negative SRCs indicating inverse relationships. The coefficient of determination (R^2) was used to check the assumption of linearity, so low R^2 indicates unreliable SRCs.

2.3.2. *Extended Fourier Amplitude Sensitivity Test (EFAST)*

The Fourier Amplitude Sensitivity Test (FAST) is a variance-based method developed by Cukier et al. (1973) for sensitivity and uncertainty analysis. The FAST method does not require any assumption of linearity and is based on the exploration of the entire parameter space by an efficient search curve; it is able to obtain the direct influence of each parameter in the total variance (first-order indices, S_i). The EFAST (Saltelli et al. 1999), which is an improvement of the FAST method, is used in the current global SA to estimate both the main effect (S_i) as well as the total effect sensitivity indices (S_{Ti}), which include all its interactions with other factors at any order. S_i and S_{Ti} are obtained as:

$$S_i = \frac{var_{x_i}[E_{x_{-i}}(Y|x_i)]}{var(Y)}$$

(10)

$$S_{Ti} = 1 - \frac{var_{x_{-i}}[Ex_i(Y|x_{-i})]}{var(Y)}$$

(11)

where var is the variance, *E* is the expected value, *Y* the model output, and x_i and x_{-i} indicate, respectively, that the operator is either applied over the ith factor or over all of them except the ith factor. The interaction between factors are therefore represented by the difference between S_{Ti} and S_i.

2.4. Local sensitivity analysis

In a regular field application, it is not possible to measure all the input variables as accurately as in a laboratory facility, especially considering the randomness and variability in the sediment build-up. Therefore, a local SA was carried out including all the model input factors, not only the H-R parameters, to ensure the transferability of the results to real catchments and to analyze the relative importance of hydraulic parameters and variables, initial sediment conditions and H-R parameters in the model outputs. The thirteen input factors considered in the local SA are those described in Section 2.1 plus a uniformity coefficient (UC), which considers the uncertainties in the spatial distribution of the initial sediment load over the street surface. This coefficient varies linearly the distribution of the initial load of sediment among the four predefined zones shown in Figure 1, taking a value of zero when all the sediment is placed in the area attached to the curb, and a value of one for a spatially uniform distribution. In our experiments the UC is 0.32.

Performing a variance-based method that considers all the variables was impossible due to the computational expense of the model. Thus, the Elementary Effects (EE) method (Saltelli et al. 2008, Campolongo et al 2007, Morris 1991), also known as the Morris screening method, was chosen following Saltelli and Annoni (2010). This method is based on the evaluation of the model along a determined number of trajectories (r) where the different factors are changed in a one-at-a-time (OAT) experimental design. Considering a model of k independent inputs $X_i, i = 1, \ldots, k$, each input is assumed to vary in the k-dimensional unitary hypercube across p selected levels. This means that the input space is discretized into a p–level grid (Ω). The ranges of the factors are assumed to be normalized for sampling, and the actual values are then calculated for simulations. The elementary effect (EE_i) for a given X_i in the output Y is defined as:

$$EE_i = \left(Y(X_1, \ldots, X_i + \Delta, \ldots, X_k) - Y(X_1, \ldots, X_i, \ldots, X_k)\right)/\Delta \quad (10)$$

where Δ is the distance between two realizations of factor X_i (inside Ω). The starting point and the order and direction in which the inputs are evaluated OAT change randomly between the different trajectories. Therefore, the mean of the absolute values of all the elementary effects obtained in each trajectory (μ*) and their standard deviation (σ) are the sensitivity measures for each input. μ^* indicates the overall influence of the factors on the output and σ estimates the variability of the EE and thus the dependency with respect to the rest of the factors.

2.5. Variables and parameters ranges

2.5.1. *Global sensitivity analysis*

Given the lack of work using the H-R model in urban catchments, which is limited to the studies presented in Hong et al. (2016a,2016b, 2019), the range of variation of the H-R parameters for the global SA (Table 2) was determined by taking into account previous erosion studies (Proffit et al. 1991, 1993, Beuselinck et al. 2002, Shaw et al. 2006, Sander et al. 2007, Heng et al. 2011 and Cea et al. 2016) and thus seeking to cover the complete performance range of the model.

2.5.2. *Local sensitivity analysis*

Table 3 shows the range of variation of the hydrodynamic variables and parameters and the initial sediment conditions used in the local SA. The ranges were centered according to the experimental layouts and their size was defined following the methodology presented in Brun et al. (2002). The input factors were classified on three levels corresponding to the degree of knowledge available in a typical field study. A relative uncertainty of 5 % (accurately known, level 1), 20 % (inaccurate known, level

2) and 50 % (very poorly known, level 3) was assigned to each level, respectively. In this way, as shown in Table 3, the hydrodynamic factors were considered as level 1. Due to the randomness and variability in the build-up and wash-off processes, the sediment diameter and the initial deposited mass and distribution of solids were defined as very poorly known variables (level 3). The sediment density was considered as a moderately inaccurate known variable (level 2), given its lower associated uncertainty.

The ranges of the H-R parameters for the local SA (Table 4) represent the uncertainty in the estimation of these parameters in order to compare the relative importance of their correct determination with respect to the hydraulic and initial sediment conditions inputs. The ranges have been defined from the global SA simulations as the interquartile ranges of the parameter sets whose total washed-off mass results differed by less than 5% from the experimental measurement.

2.6. Implementation

The selected SA methods and metrics have been conditioned by the computationally expensive model. The model is solved using the explicit finite volume solver presented in Cea and Vázquez-Cendón (2012) and compiled for a Windows environment. Each simulation takes about five minutes using an Intel® Core i5-7500 3.4 GHz computer. The methodology implementing the different sensitivity methods and the number of simulations performed for each analysis are included in the following sections.

2.6.1. *Standardized regression coefficients*

Regarding the SRC, the Latin Hypercube Sampling (LHS) method was used to generate 1000 sets of H-R parameters for each of the twelve laboratory experiments, and considering the ranges of variation established in Table 2, using the free Matlab toolbox SAFE (Pianosi et al. 2015). Then, the multiple linear regressions were obtained by means of the *regress* function in Matlab. Convergence test considering 100, 500, 1000, 2000 and 5000 simulations showed that convergence was achieved with a sample size of 1000 simulations. Thus, over the twelve laboratory experiments, the total number of simulations was 12000.

2.6.2. E*xtended Fourier amplitude sensitivity test*

The toolbox Eikos, developed by Ekstrom (2005), was used for the calculation of the EFAST indices and for the sampling process, taking into account the ranges defined in Table 2. Due to the computational cost of the wash-off model, the number of simulations used for the implementation of the EFAST method was set to 505 per factor (3030 simulations per laboratory experiment and a total of 36360), which remains within the practical recommendations accordingly to Saltelli et al. (2005) and Cosenza et al (2013).

2.6.3. *Elementary effects*

Following Campolongo and Saltelli (1997), Campolongo et al. (1999) and Saltelli et al. (2000), a number of trajectories r=10 and values of p=4 ({0, 1/3, 2/3, 1}) and Δ=2/3 were chosen in the implementation of the EE method. In order to facilitate a better coverage of the input domain, these ten trajectories were selected from a set of twenty-five, which effectively maximizes their spread in the input space (Campolongo et al. 2007). The local SA assessed thirteen inputs, so the number of simulations was 10(13+1)=140 for each laboratory experiment, a total of 1680 simulations.

2.7. Assessment of model predictions

In order to analyze the model performance, we first compared predictions with the results of the laboratory experiments, using the mean of the Nash-Sutcliffe model efficiency coefficient (NSE) in each of the gully pots as an objective function to assess overall prediction performance. Second, we checked the adequacy of the ranges selected for the global SA by visual assessment of the contours of the results of simulations. Although Root-Mean-Squared-Deviation (RMSE) or NSE can be used as objective functions to assess model sensitivity (Hong et al. 2016a), in the light of the model performance observed, we chose the TSS concentration peaks and the washed-off loads as outputs to analyze. These two outputs are the most significant ones for practitioners, since they are relevant variables for estimating the impacts of the stormwater pollution inflows to sewerage systems or the aquatic media.

3. RESULTS

3.1. Model and ranges performance

To assess the suitability of model predictions, Figure 3 shows two examples of the five best TSS with rain intensities of 50 and 80 mm/h and sediment classes D2 and D3, respectively. It can be seen that the flexibility of the model and the established ranges allow for an accurate prediction of the TSS pollutographs in both gully pots at the same time and for both initial conditions. In addition, the parameter sets of the five best-fitted predictions performed for the global SA are also included in Figure 3. It can be seen that, as expected, different sets of parameters resulted in very similar pollutographs.

3.2. Global sensitivity analysis

3.2.1. *Standardized Regression Coefficients (SRC)*

The SRC of the six H-R parameters regarding the total washed-off mass and the TSS peak for each gully pot are shown in Figure 4. The plots show the sensitivity indices of each parameter for the twelve laboratory experiments that have been used as layouts for the SA, considering the three different rain intensities and the four sediment grain sizes described above (Section 2.2).

In general, the plots in Figure 4 show the critical mass (Ms_{cr}) as the most important H-R parameter, with the highest influence in both outputs and for all the laboratory experiments. The critical mass is the mass required to reach the total rain-driven and flow-driven potential detachment, so its effect on the results is increased in urban catchments due to the scattering of sediment when low loads are presented over the street. In addition, the relative importance of the H-R parameters varies widely with respect to the grain size, and b and Ω_0 remain with a low influence in both outputs and for all the laboratory experiments.

Looking at the total washed-off mass sensitivity results in Figure 4 (first row plots), it can be seen that as the grain size of the sediment increases, the influence of the rain-driven detachment parameters α_0 and h_0 decrease and F becomes more important. Ms_{cr}, α_0 and h_0 are thus key parameters for modelling wash-off with small grain sizes, but F has to be taken into account if bigger diameters are involved. An increase in rain intensity also involves a large increase in the sensitivity of the total washed-off mass results to h_0, which depends on the water depth. The sensitivity results for the TSS peak (second row plots in Figure 4) are very similar in terms of the main parameters and in the different laboratory experiments analyzed. However, h_0 and b become wholly negligible to the results, since h_0 is the water depth threshold from which the rain-driven detachment is dumped, thus the TSS peak, which is produced at the beginning of the rain event, and is not affected.

Another interesting result in Figure 4 is the high match between the sensitivity results of both gully-pots. Despite gully pot 2 having a far more important curb flow component, only a slight increase in the sensitivity to F and a small reduction in the sensitivity to α_0 and h_0 were observed for gully pot 2. Finally, it should be noted that the coefficients of determination obtained in the regressions, with values between 0.5 and 0.85 in the total mass and between 0.35 and 0.6 in the TSS peak, indicate that a significant part of the variance is not explained by a linear regression model, which cannot represent the interaction between model parameters. In sum,α_0, h_0, Ms_{cr} and F appeared to be the important parameters for the washed-off mass, and only α_0, Ms_{cr} and F for the TSS concentration peak. In addition, the rain and flow-driven detachment parameters were presented as key for smaller (mean grain sizes of 30 and 68 μm) and larger (144 and 274 μm) sediment particles, respectively

3.2.2 *Extended Fourier Amplitude Sensitivity Test (EFAST)*

In contrast to SRC, the EFAST method considers the interactions between the different parameters. Figure 5 shows the direct or first order effect and the total effect of the H-R parameters in the total washed-off mass and the TSS peak, computed with the EFAST methodology. Despite the fact that the coefficients of determination in the SRC analysis indicated in the same cases low reliability, with values below 0.6, the ranking of the most important parameters considering the first order effect results is very similar, as was also found in Cosenza et al. (2013). In addition, variations in the first order indices due to the changes of the sediment diameter and rain intensity in the different laboratory experiments show the same trends as in the SRC.

The critical mass (Ms_{cr}) is the most important H-R parameter for all the laboratory experiments in the plots presented in Figure 5. Regarding the total washed-off mass results (first row plots in Figure 5), α_0 and h_0 are at a secondary level, with only a low degree of influence, including F in the case of the larger grain sizes (sediment classes 3 and 4). b and Ω_0 appear to be negligible parameters for all the laboratory experiments analysed. In addition, some differences in the EFAST indices between both gully pots should be noted: α_0 and h_0 decrease and F increases their influence in the results for gully pot 2, which has an important curb flow component. Considering the sensitivities of the TSS peak to the parameters (second row plots in Figure 5), the flow-driven detachment parameters F and Ω_0 are low influential parameters, the rest of the rain-driven detachment parameters, α_0, h_0 and b, being negligible.

The differences between the total (bars with light colors) and first order effect indices (bars with dark colors) in the plots in Figure 5 show the variance of the results due to interactions between parameters. It can be seen that the interactions play an important role in the results, especially in the TSS peak concentration and in the larger diameters (sediment classes 3 and 4) for the total washed-off mass. Unfortunately, this complicates the separation of the individual effect of each parameter and confirms our expectations that it is indeed challenging to calibrate this model. Summarizing, washed-off mass and TSS peak are very sensitivity to Ms_{cr} in all the experimental layouts. The same trends as in SRC have been observed between the relative importance of rain-driven and flow-driven detachment parameters and rain intensity and grain size values. In addition, a high level of interaction between parameters was found.

3.3. Local sensitivity analysis

Figure 6 shows the absolute mean (μ^*) of the elementary effects of each input factor with respect to the total washed-off mass against their standard deviation (σ) for the twelve laboratory experiments. The relation between μ^* and σ is an indicator of the linearity of each variable with respect to the model output, assuming that below 0.1 there are no substantial interactions with other factors. Only the results corresponding to the gully pot 2 are plotted here, but similar results are obtained for the gully pot 1. The initial load of sediment over the surface (Ms_0) and its mean diameter (D_{50}), classified as very poorly known variables, are the most influential measurable variables in all cases. The influence of the density is lower than that of the sediment diameter, although both variables affect the settling velocity of the solid particles. This is because its associated uncertainty is lower.

The other input factor that shows a notable influence in the results is critical mass (Ms_{cr}), which was identified as the most influential H-R parameter in the global SA. Regarding the rest of the H-R parameters, their relative importance is the same in both the SRC and the EFAST analyses. Thus, the influence of α_0 and h_0 is higher for the particles with lower diameters (sediment classes 1 and 2) and decreases as the sediment diameter increases. The influence of the uniformity coefficient (UC) is low in all cases, despite its high level of uncertainty, which allows us to conclude that the differences in sediment distribution considered do not substantially affect the total washed-off mass. This confirms the findings of Naves et al. (2017). The hydraulic variables and parameters remain with the lowest influence on the results, mainly because of the low uncertainties associated with these.

The local sensitivity results regarding the TSS peak concentration in gully pot 2 for all the laboratory experiments are included in Figure 7. The input factors with most influence in the TSS peak are the same three factors (Ms_0, D_{50} and Ms_{cr}) as in the case of the total washed-off mass. However, the H-R parameters related to the flow-driven detachment, especially F, are at a similar level of importance for the TSS peak. Thus, as seen in the global SA, the flow-driven detachment is key to accurately modelling the maximum TSS concentration. The hydraulic input factors and the rain-driven detachment parameters seem to be almost negligible for this output.

In sum, our findings suggest that the initial load of sediment and the mean grain size were the most important variables. H-R parameters exhibited a high influence in the model outputs, with a similar behavior to that observed in the global SA. Finally, hydraulic input factors variations do not affect the outputs, since their determination has a low degree of uncertainty associated with it.

4. DISCUSSION

In the previous sections, we have presented a SA of a physically-based urban wash-off model. The study has shown that the flexibility of the model allowed for the replication of the laboratory results from accurately measured initial conditions by tuning the H-R model parameters. However, this flexibility also leads to identifiability problems and makes it difficult to obtain precise predictions in field studies. Therefore, it is important to discuss our findings in terms of: i) a careful interpretation of the SA results, ii) transferability to field studies, and iii) limitations and future steps towards improving urban wash-off predictions.

4.1. Interpretation of the sensitivity analysis results

Uncertainties and interactions between the different processes involved in wash-off modelling such as flow and rain characterization, model parameters, or sediment initial conditions and characteristics, make it difficult to separate their individual contribution to a model's predictions. Therefore, controlled laboratory experiments have been used to eliminate disturbances and to focus the global SA on the H-R model parameters, fixing remaining input variables. However, despite the accurate definition of the initial conditions, Figure 3 shown a wide range of possible model predictions that might alter the H-R parameters. This is a consequence of a lack of knowledge in estimating their possible values in urban catchments. In addition, there is no consensus as to model simplifications in the literature and, to date, it is difficult to define narrower ranges a priori. However, using the obtained global SA results, it is possible to address this lack of knowledge and identifiability issues, and thus to reduce the number of parameters to calibrate in future research.

While flow-driven detachment is usually negligible in soil erosion (Cea et al. 2016), it was seen as an important process for the largest grain sizes (144 and 274 μm) in our urban application. Therefore, rain-driven and flow-driven detachment are the two physical processes that have to be taken into account using the H-R parameters. Regarding rain-driven detachment, exponent b is negligible for all the laboratory experiments that we simulated, so its value could be fixed at 1. The water depth damping threshold, h_0, is typically set to two third of the mean raindrop size (Heng et al. 2011, Hong et al. 2016a). However, its high influence in modelling TSS peak concentrations, as well as the current lack of studies accurately measuring rain drop size distributions (DSD), mean that the development of work aimed at adequately fixing this parameter is an interesting line of research. With respect to the flow-driven parameters, Ω_0 showed a low influence in the results and may be fixed to values around 0.01 W/m^{2,} following previous studies (Proffitt et al. 1993, Sander et al. 2007, Heng et al. 2011).

Two processes must be adjusted by the remainder H-R model parameters: rain- and flow-driven detachment of particles. Among these three parameters (α_0, Ms_{cr} and F), which are those with the highest influence in the results, Ms_{cr} affects both processes at the same time, and may be fixed in future applications. However, due to the current lack of knowledge on this parameter, its notable influence in the results, plus its interactions with other parameters, this is not currently recommended. Therefore, given the sensitivity results, we proposed in this section a reduction from 6 to 3 calibration parameters. However, next field and laboratory urban wash-off studies will increase our understanding of the H-R parameters, and may lead to a reduction in parameter ranges and to a consideration of further simplifications.

4.2. Transferability to field studies

When applying the H-R model in real-world catchments, we currently see three main limitations: i) high computational cost, ii) inaccurate input variables, and iii) the consideration of sediment heterogeneity.

The model was already previously calibrated for different rain events in a 2661 m^2 road urban catchment in Hong et al. (2016a, 2016b, 2019). This work is the first and available field application of H-R model in urban environments, and studies in larger field catchments are currently challenging due to the mentioned limitations. However, physical-based wash-off models are at the beginning of their development and can be compared to 2D flood models in the early 2000s, when their applicability to large catchments were limited because computers were still slow and high-resolution terrain models were missing. In the same way as 2D-1D coupling is currently industry standard in urban drainage models, we think that the limitations in the catchment size for urban wash-off physically-based models will be significantly decreased in the near future and this will highlight, also for large catchments, the opportunities raised by physically-based wash-off models. In this regard, the 2D shallow water model Iber has recently been improved, and now takes advantage of the parallelization functionalities of both CPUs (central processing units) and GPUs (graphics processing units), achieving speedups of up to two orders of magnitude in comparison with the version used in the present study (García-Feal et al. 2018). In addition, the use of fast emulators has already been applied in hydrodynamic urban drainage models (Carbajal et al. 2017, Hong et al. 2019), and these might be a very practical solution to reduce the computation time. Meanwhile, the application of physically-based wash-off models to small and medium-size basins is an opportunity to increase understanding of wash-off process and model performance.

Regarding the definition of input variables, as shown by the local SA, the initial load of sediment and mean grain size are the most important input variables in terms of model's predictions, as also found in Hong et al. (2016a). Therefore, the uncertainties associated with these variables due to the variability and randomness of sediment build-up can limit the reliability of the results and make the model ineffective. The determination of the initial conditions, then, is key to the modelling of urban wash-off, and future research should continue to be oriented towards the determination of the initial build-up mass and characteristics, either through field studies analyzing urban dust samples (Wijesiri et al. 2015b) or by following the ideas in Sandoval et al. (2018) where input variables are estimated from measured pollutographs using virtual state variables.

Spatial heterogeneity is other important issue to consider in terms of the transferability of the model. First, an accurate representation of the surface flow is needed to reduce the propagation of hydraulic uncertainties to the sediment transport equations, since the hydrodynamic model is used as a basis for wash-off equations. Visualization techniques such as large-scale particle image velocimetry (LSPIV) or surface structure image velocimetry (SSIV) can help to achieve the required accuracy here by obtaining useful surface calibration data (Naves 2019b), with the possibility of using surveillance camera footage, as proposed in Leitão et al. (2018). The accuracy and resolution of elevation data are also key to attaining a suitable characterization of surface flow. However, current LIDAR techniques are able to provide high-resolution elevations each 0.1 m which, combined with manual measurements to incorporate important elements such as curbs, have demonstrated their effectiveness in representing adequately flow spatial variations (Hong et al. 2016a, b). In addition, gully pots and grid performance should be also included at this level of detail. In fact, this is interesting not only for surface flow modelling (Martins et al 2018) but also for water quality interactions and gully pot efficiency (Post et al. 2016).

Rainfall input data involves spatial intensity distribution, which allows for obtaining an accurate surface flow, as well as rain energy, which depends on DSD and condition rain-driven detachment. An extensive literature exists on rain distribution and resolution in hydrological processes, but future research in urban wash-off should incorporate DSD measurements more frequently, in order to estimate rain-driven particle detachment from rain kinetic energy. Rainfall simulators, such as the one used in this study, can contribute to an understanding of this process through the use of constant rain intensities and varying DSDs.

Finally, it is necessary to take into account the heterogeneity in the surface sediment mass. In the laboratory experiments described here, there are four different sediment classes with a uniform granulometry, this as a means of achieving greater control of the process. However, available surface sediment presents a high degree of heterogeneity in grain sizes and densities in real catchments, and mean diameter and density are not representative. In addition, representative characteristics of the sediment can change during the event as the lightest particles are washed-off first. A multiclass approach, such as the one used in Hong et al. (2016b), should therefore be considered as a means of obtaining reliable results with heterogeneous sediment masses. This approach leads to an increase in the complexity of the model, with adequate parameters needed for each class, and hence an assessment of the benefits and drawbacks that such an approximation might involve would be a useful step. In this regard, the experimental data set used in this study (which is taken from the dataset Naves et al. 2019a) also includes experiments where the four sediment classes were mixed to obtain a realistic granulometry and including coulter samples in the inflow to the gully pots, and may be used in future studies.

4.3. General perspectives for modelling urban wash-off

The future aims of wash-off modelling in urban areas should not be seek to implement more and more complex models in which all the physical processes are perfectly defined. Rather, the objective should be to move towards models capable of considering the spatial and temporal heterogeneities of the catchment and able to reproduce the key wash-off process, overcoming the limitations of empirical equations yet maintaining optimal simplicity in the model. For this purpose, more laboratory and field applications of wash-off physical-based models should be conducted to increase our understanding of the parameters and processes here, one very important focus of attention being an effective characterization of catchment, sediment and rain characteristics. The wash-off process is challenging, but in view of the promising results of the first physically-based wash-off studies, it is an important line of research towards better treatment and management techniques for minimizing the impact of urban surface contaminants, such as microplastics, heavy metals and PAH, on the environments of cities and towns.

5. CONCLUSIONS

This study contributes to the understanding of physically-based urban wash-off models by presenting an in-depth SA using a series of specially-tailored laboratory experiments obtained on a realistic and 1:1 scale rainfall simulator of 36 m^2. Thus, the accurate determination of the hydraulics variables and the initial sediment conditions were used to focus a global SA on poorly-known H-R parameters using SRC and

EFAST methods. Then, in order to ensure the transferability of the results to field studies, the relative importance in the model outputs of hydraulic parameters, initial sediment conditions and H-R model parameters was assessed through a local SA, using the EE method and considering uncertainties in their determination in real field studies. Specifically, the following can be concluded based on the results:

- The flexibility of the model allowed us to successfully reproduce the results of the laboratory experiments by tuning the H-R model parameters. However, the predictions obtained suggested a complex calibration process, and thus highlight the usefulness of the SA performed for decision-making in order to simplify the model and to deal with identifiability problems.
- The SRC indicated a strong sensitivity of the results to critical mass in comparison to the other H-R parameters. The parameters related to rain-driven detachment α_0 and h_0 were at a second level of importance, roughly half that of sensitivity, for the total washed-off mass with the smallest diameters (mean grain sizes of 30 and 68 μm). When the grain size of the sediment increased (144 and 274 μm), F was included in this second level of influence. In addition, F was also shown to be an important variable with respect to the TSS peak, while b and Ω_0 remained at a low influence for both outputs.
- Although the ranking of the most important parameters obtained from the EFAST analysis was very similar to that for the SRC results, the EFAST total effect indices revealed the high importance of the interaction between parameters in the model outputs, which is also an indicator of the difficulties that can arise when calibrating the model.
- In the local SA, which considered all the input variables and parameters, the initial load of sediment, mean grain size and critical mass were seen to be the most important factors for the total washed-off mass and the TSS peak in all the laboratory experiments. Therefore, very accurate measurement of the available mass and its characteristics is necessary in order to avoid the variability

associated with the build-up process affecting to the reliability of results. H-R parameters were seen to be at a second level of importance, which illustrates the need for accurate calibration of the model. Finally, variations in hydraulic variables did not affect the outputs since the uncertainty associated with their determination was low.

- In the light of these results, the model may be simplified using the three parameters with the highest influence in the results, α_0, Ms_{cr} and F, as a means of modelling the individual contribution of the rain-driven and flow-driven detachment. Future research should focus on more laboratory and field studies, to increase our knowledge of H-R parameters and thus to be able to adequately fix them.

Although the problem is complex, these promising results should stimulate efforts towards overcoming the current limitations of physically-based models, such as high computational cost, the need for an accurate definition of the input variables, and the accurate modelling of spatial and sediment heterogeneities.

Acknowledgments

The first author was in receipt of a predoctoral grant [FPU14/01778] and an internship fellowship to visit the EAWAG [EST17/00715], from the Spanish Ministry of Science, Innovation and Universities. The authors would also like to acknowledge fruitful discussions with Andreas Scheidegger and Juan Pablo Carbajal.

References

Akan, A. O. Houghtalen, R. J., (2003). Urban hydrology, hydraulics, and stormwater quality: engineering applications and computer modeling. John Wiley & Sons.

Anta, J., Peña, E., Suárez, J., Cagiao, J. (2006). A BMP selection process based on the granulometry of runoff solids in a separate urban catchment. Water Sa, 32(3), 419-428. http://dx.doi.org/10.4314/wsa.v32i3.5268

Beuselinck, L., Govers, G., Hairsine, P. B., Sander, G. C., Breynaert, M. (2002). The influence of rainfall on sediment transport by overland flow over areas of net deposition. Journal of Hydrology, 257(1-4), 145-163. https://doi.org/10.1016/S0022-1694(01)00548-0

Bladé, E., Cea, L., Corestein, G., Escolano, E., Puertas, J., Vázquez-Cendón, E., Dolz, J., Coll, A. (2014). Iber: herramienta de simulación numérica del flujo en ríos. Revista Internacional de Métodos Numéricos para Cálculo y Diseño en Ingeniería, 30(1), 1-10. https://doi.org/10.1016/j.rimni.2012.07.004

Butler, D., Davies, J. (2010) Urban Drainage, 3rd edn. Spon Press, Abingdon, UK

Brun, R., Kühni, M., Siegrist, H., Gujer, W., Reichert, P. (2002). Practical identifiability of ASM2d parameters—systematic selection and tuning of parameter subsets. Water research, 36(16), 4113-4127. https://doi.org/10.1016/S0043-1354(02)00104-5

Campolongo, F., Saltelli, A., (1997). Sensitivity analysis of an environmental model: a worked application of different analysis methods. Reliability Engineering and System Safety 52, 49–69. https://doi.org/10.1016/S0951-8320(97)00021-5

Campolongo, F., Tarantola, S., Saltelli, A. (1999). Tackling quantitatively large dimensionality problems. Computer Physics Communications 117, 75–85. https://doi.org/10.1016/S0010-4655(98)00165-9

Campolongo, F., Cariboni, J., Saltelli, A. (2007). An effective screening design for sensitivity analysis of large models. Environmental Modelling and Software 22, 1509–1518. https://doi.org/10.1016/j.envsoft.2006.10.004

Carbajal, J. P., Leitão, J. P., Albert, C., & Rieckermann, J. (2017). Appraisal of data-driven and mechanistic emulators of nonlinear simulators: The case of hydrodynamic urban drainage models. Environmental modelling & software, 92, 17-27. https://doi.org/10.1016/j.envsoft.2017.02.006

Cea, L., Garrido, M., Puertas, J., (2010). Experimental validation of two-dimensional depth-averaged models for forecasting rainfall–runoff from precipitation data in urban areas. J. Hydrol. 382 (1), 88–102. https://doi.org/10.1016/j.jhydrol.2009.12.020

Cea, L., Vázquez-Cendón, M. E. (2012). Unstructured finite volume discretisation of bed friction and convective flux in solute transport models linked to the shallow water equations. Journal of Computational Physics, 231(8), 3317-3339. https://doi.org/10.1016/j.jcp.2012.01.007

Cea, L., Blade, E., (2015). A simple and efficient unstructured finite volume scheme for solving the shallow water equations in overland flow applications. Water Resour. Res. 51 (7), 5464–5486. https://doi.org/10.1002/2014WR016547

Cea, L., Legout, C., Grangeon, T., Nord, G. (2016). Impact of model simplifications on soil erosion predictions: application of the GLUE methodology to a distributed event-based model at the hillslope scale. Hydrological Processes, 30(7), 1096-1113. https://doi.org/10.1002/hyp.10697

Cosenza, A., Mannina, G., Vanrolleghem, P. A., Neumann, M. B. (2013). Global sensitivity analysis in wastewater applications: A comprehensive comparison of different methods. Environmental modelling & software, 49, 40-52. https://doi.org/10.1016/j.envsoft.2013.07.009

Cukier, R. I., Fortuin, C. M., Shuler, K. E., Petschek, A. G., Schaibly, J. H. (1973). Study of the sensitivity of coupled reaction systems to uncertainties in rate coefficients. I Theory. The Journal of chemical physics, 59(8), 3873-3878. https://doi.org/10.1063/1.1680571

Deletic, A., Maksimovic, E., Ivetic, M. (1997). Modelling of storm wash-off of suspended solids from impervious surfaces. Journal of Hydraulic Research, 35(1), 99-118. https://doi.org/10.1080/00221689709498646

Deletic, A., Orr, D.W. (2005). Pollution buildup on road surfaces. Journal of Environmental Engineering, 131(1), 49-59. https://doi.org/10.1061/(ASCE)0733-9372(2005)131:1(49)

Dehghani, S., Moore, F., Akhbarizadeh, R. (2017). Microplastic pollution in deposited urban dust, Tehran metropolis, Iran. Environmental Science and Pollution Research, 24(25), 20360-20371. http://doi.org/10.1007/s11356-017-9674-1

Donckels, B.M.R., Kroll, S., Van Dorpe, M., & Weemaes, M. (2014). Global sensitivity analysis of an in-sewer process model for the study of sulfide-induced corrosion of concrete. Water Science and Technology, 69(3), 647-655. http://doi.org/10.2166/wst.2013.763

Dris, R., Gasperi, J., Rocher, V., Saad, M., Renault, N., Tassin, B. (2015). Microplastic contamination in an urban area: a case study in Greater Paris. Environmental Chemistry, 12(5), 592-599. http://doi.org/10.1071/EN14167

Ekstrom, P.A. (2005). Eikos: a simulation toolbox for sensitivity analysis in matlab. Uppsala University, Uppsala

Egodawatta, P., Thomas, E., Goonetilleke, A., (2007). Mathematical interpretation of pollutant wash-off from urban road surfaces using simulated rainfall. Water Res. 41 (13), 3025–3031. https://doi.org/10.1016/j.watres.2007.03.037.

Fraga, I., Cea, L., Puertas, J., (2015). Validation of a 1D-2D dual drainage model under unsteady part-full and surcharged sewer conditions, Urban Water J. 14 (1), 74–84. https://doi.org/10.1080/1573062X.2015.1057180

Fraga, I., Cea, L., Puertas, J., Suárez, J., Jiménez, V., Jácome, A., (2016). Global Sensitivity and GLUE-Based Uncertainty Analysis of a 2D-1D Dual Urban Drainage Model. J. Hydrol. Eng. 21 (5), 04016004. https://doi.org/10.1061/(asce)he.1943-5584.0001335

Gamerith, V., Neumann, M.B., & Muschalla, D. (2013). Applying global sensitivity analysis to the modelling of flow and water quality in sewers. Water research, 47(13), 4600-4611. http://dx.doi.org/10.1016/j.watres.2013.04.054

Gao, B., Walter, M.T., Steenhuis, T.S., Parlange, J.Y., Nakano, K., Hogarth, W.L., Rose, C. (2003) Investigating ponding depth and soil detachability for a mechanistic erosion model using a simple experiment. Journal of Hydrology277(1–2): 116–124. https://doi.org/ 10.1016/S0022-1694(03)00085-4

García-Feal, O., González-Cao, J., Gómez-Gesteira, M., Cea, L., Domínguez, J., Formella, A. (2018). An accelerated tool for flood modelling based on Iber. Water, 10(10), 1459. https://doi.org/10.3390/w10101459

Gorgoglione, A., Bombardelli, F.A., Pitton, B.J., Oki, L.R., Haver, D.L., Young, T.M. (2019). Uncertainty in the parameterization of sediment build-up and wash-off processes in the simulation of sediment transport in urban areas. Environ. Modell. Softw., 111, 170-181. https://doi.org/10.1016/j.envsoft.2018.09.022

Grottker, M. (1987). Runoff quality from a street with medium traffic loading. Science of the Total Environment, 59, 457-466. https://doi.org/10.1016/0048-9697(87)90469-4

Hairsine, P.B., Rose, C.W., (1992a). Modeling water erosion due to overland flow using physical principles: 1. Sheet flow. Water Resour. Res. 28, 237–243. http://doi.org/10.1029/91wr02380.

Hairsine, P.B., Rose, C.W., (1992b). Modeling water erosion due to overland flow using physical principles: 2. Rill flow. Water Resour. Res. 28, 245–250. http://doi.org/10.1029/91wr02381.

Helton, J. C. (1993). Uncertainty and sensitivity analysis techniques for use in performance assessment for radioactive waste disposal. Reliability Engineering & System Safety, 42(2-3), 327-367. https://doi.org/10.1016/0951-8320(93)90097-I

Heng, B. C. P., G. C. Sander, A. Armstrong, J. N. Quinton, J. H. Chandler, and C. F. Scott (2011), Modeling the dynamics of soil erosion and size-selective sediment transport over nonuniform topography in flume-scale experiments, Water Resour. Res., 47, W02513. https://doi.org/10.1029/2010WR009375

Herngren, L. F., (2005). Build-up and Wash-off Process Kinetics of PAHs and Heavy Metals on Paved Surfaces Using Simulated Rainfall. Doctoral dissertation, Queensland University of Technology, Brisbane, Queensland, Australia

Hong, M., Bonhomme, C., Le, M.H., Chebbo, G., (2016a). A new approach of monitoring and physically-based modelling to investigate urban wash-off process on a road catchment near Paris. Water Res. 102, 96–108, https://doi.org/10.1016/j.watres.2016.06.027

Hong, M., Bonhomme, C., Le, M.H., Chebbo, G., (2016b). New insights into the urban washoff process with detailed physical modelling. Sci. Total Environ. 573, 924–936. https://doi.org/10.1016/j.scitotenv.2016.08.193

Hong, Y., Liao, Q., Bonhomme, C., Chebbo, G. (2019). Physically-based urban stormwater quality modelling: An efficient approach for calibration and sensitivity analysis. Journal of environmental management, 246, 462-471.

Julien, P. Y. (2010). Erosion and sedimentation. Cambridge University Press, Cambridge.

Leitão, J.P., Peña-Haro, S., Lüthi, B., Scheidegger, A., de Vitry, M.M., 2018. Urban overland runoff velocity measurement with consumer-grade surveillance cameras and surface structure image velocimetry. J. Hydrol. 565, 791–804. https://doi.org/10.1016/j.jhydrol.2018.09.001.

Leutnant, D., Muschalla, D., Uhl, M. (2018). Statistical distribution of TSS event loads from small urban environments. Water, 10(6), 769. https://doi.org/10.3390/w10060769

Mannina, G., Cosenza, A., Gori, R., Garrido-Baserbac, M., Sobhani, R., & Rosso, D. (2016). Greenhouse gas emissions from wastewater treatment plants on a plantwide scale: sensitivity and uncertainty analysis. Journal of Environmental Engineering, 142(6), 04016017. https://doi.org/10.1061/ (ASCE)EE.1943-7870.0001082

Martins, R., Rubinato, M., Kesserwani, G., Leandro, J., Djordjević, S., & Shucksmith, J. D. (2018). On the Characteristics of Velocities Fields in the Vicinity of Manhole Inlet Grates During Flood Events. Water Resources Research, 54(9), 6408-6422. https://doi.org/10.1029/2018WR022782

Massoudieh, A., Abrishamchi, A., Kayhanian, M. (2008). Mathematical modeling of first flush in highway storm runoff using genetic algorithm. Science of the total environment, 398(1-3), 107-121. https://doi.org/10.1016/j.scitotenv.2008.02.050

Morris, M. D. (1991). Factorial sampling plans for preliminary computational experiments. Technometrics 33, 161–174.

Muthusamy, M., Tait, S., Schellart, A., Beg, M.N.A., Carvalho, F.R. de Lima, J.L.M.P., (2018). Improving understanding of the underlying physical process of sediment wash-off from urban road surfaces. J. Hydrol. 557, 426–433, https://doi.org/10.1016/j.jhydrol.2017.11.047.

Naves, J., Jikia, Z., Anta, J., Puertas, J., Suárez, J., Regueiro-Picallo, M., (2017). Experimental study of pollutant washoff on a full-scale street section physical model. Water Sci. Technol. 76 (10), 2821–2829. https://doi.org/10.2166/wst.2017.345.

[dataset] Naves, J., Puertas, J., Suárez, J., Anta, J. (2019a) WASHTREET project experimental data. Zenodo. http://doi.org/10.5281/zenodo.3233918

Naves, J., Anta J., Puertas J., Regueiro-Picallo, M., Suárez, J. (2019b) Using a 2D shallow waters model to assess Large-scale Particle Image Velocimetry (LSPIV) and Structure from Motion (SfM) techniques in a street-scale urban drainage physical model. Journal of Hydrology 575, 54-65 https://doi.org/10.1016/j.jhydrol.2019.05.003

Pianosi, F., Sarrazin, F., Wagener, T. (2015). A Matlab toolbox for global sensitivity analysis. Environmental Modelling & Software, 70, 80-85. https://doi.org/10.1016/j.envsoft.2015.04.009

Pitt, R., Williamson, D., Voorhees, J., Clark, S. (2004). Review of historical street dust and dirt accumulation and washoff data. Effective Modeling of Urban Water Systems, Monograph, 13, 43-54. https://doi.org/10.14796/JWMM.R223-12

Post, J. A. B., Pothof, I. W. M., Dirksen, J., Baars, E. J., Langeveld, J. G., & Clemens, F. H. L. R. (2016). Monitoring and statistical modelling of sedimentation in gully pots. Water research, 88, 245-256. https://doi.org/10.1016/j.watres.2015.10.021

Proffitt, A. P. B., Rose, C. W., Hairsine, P. B. (1991). Rainfall detachment and deposition: Experiments with low slopes and significant water depths. Soil Science

Society of America Journal, 55(2), 325-332. https://doi.org/10.2136/sssaj1991.03615995005500020004x

Proffitt, A. P. B., Hairsine, P. B., Rose, C. W. (1993). Modeling soil erosion by overland flow: application over a range of hydraulic conditions. Transactions of the ASAE, 36(6), 1743-1753. https://doi.org/10.13031/2013.28519

Rijn, L. C. V. (1984). Sediment transport, part II: suspended load transport. Journal of hydraulic engineering, 110(11), 1613-1641. https://doi.org/10.1061/(ASCE)0733-9429(1984)110:11(1613)

Rossi, L., Chèvre, N., Fankhauser, R., Krejci, V. (2009). Probabilistic environmental risk assessment of urban wet-weather discharges: an approach developed for Switzerland. Urban Water Journal, 6(5), 355-367. https://doi.org/10.1080/15730620902934801

Rossman, L. A., (2015) Storm Water Management Model, User's Manual, Version 5.1 No. EPA/600/R-05/040). US Environmental Protection Agency, Cincinnati, OH, USA

Saltelli, A., Tarantola, S., Chan, K. S. (1999). A quantitative model-independent method for global sensitivity analysis of model output. Technometrics, 41(1), 39-56. https://doi.org/10.1080/00401706.1999.10485594

Saltelli, A., Chan, K., Scott, E. M. (Eds.). (2000). Sensitivity analysis (Vol. 1). New York: Wiley.

Saltelli, A., Ratto, M., Tarantola, S., Campolongo, F. (2005). Sensitivity analysis for chemical models. Chemical reviews, 105(7), 2811-2828. https://doi.org/10.1021/cr040659d

Saltelli, A., Ratto, M., Andres, T., Campolongo, F., Cariboni, J., Gatelli, D., Saisana, M., Tarantola, S. (2008). Global sensitivity analysis: the primer. John Wiley & Sons.

Saltelli, A., Annoni, P. (2010). How to avoid a perfunctory sensitivity analysis. Environmental Modelling & Software, 25(12), 1508-1517. https://doi.org/10.1016/j.envsoft.2010.04.012

Sander, G. C., Parlange, J. Y., Barry, D. A., Parlange, M. B., Hogarth, W. L. (2007). Limitation of the transport capacity approach in sediment transport modeling. Water Resources Research, 43(2). https://doi.org/10.1029/2006WR005177

Sandoval, S., Vezzaro, L., Bertrand-Krajewski, J. L. (2018). Revisiting conceptual stormwater quality models by reconstructing virtual state variables. Water Science and Technology, 78(3), 655-663. https://doi.org/10.2166/wst.2018.337

Sartor, J.D., Boyd, G.B., (1972). Water Pollution Aspects of Street Surface Contaminants. EPA-R2-72-081. United States Environmental Protection Agency, Washington, DC, USA.

Schellart, A.N.A., Tait, S.J., Ashley, R.M. (2010). Towards quantification of uncertainty in predicting water quality failures in integrated catchment model studies. Water research, 44(13), 3893-3904. https://doi.org/10.1016/j.watres.2010.05.001

Sharma, P.P., Gupta, S.C., Foster, G.R. (1993). Predicting soil detachment by raindrops. Soil Science Society of America Journal57: 674–680. https://doi.org/10.2136/sssaj1993.03615995005700030007x

Sharma, P.P., Gupta, S.C., Foster, G.R. (1995). Raindrop-induced soil detachment and sediment transport from interrill areas. Soil Science Society of America Journal59: 727–734. https://doi.org/10.2136/sssaj1995.03615995005900030014x

Shaw, S. B., Walter, M.T., Steenhuis, T.S. (2006). A physical model of particulate wash-off from rough impervious surfaces. Journal of Hydrology, 327(3-4), 618-626. https://doi.org/10.1016/j.jhydrol.2006.01.024

Shaw, S.B., Parlange, J.Y., Lebowitz, M., Walter, M.T. (2009). Accounting for surface roughness in a physically-based urban wash-off model. Journal of hydrology, 367(1-2), 79-85. https://doi.org/10.1016/j.jhydrol.2009.01.004

Sikorska, A. E., Del Giudice, D., Banasik, K., & Rieckermann, J. (2015). The value of streamflow data in improving TSS predictions–Bayesian multi-objective calibration. Journal of Hydrology, 530, 241-254. https://doi.org/10.1016/j.jhydrol.2015.09.051

Vanrolleghem, P. A., Mannina, G., Cosenza, A., Neumann, M. B. (2015). Global sensitivity analysis for urban water quality modelling: Terminology, convergence and comparison of different methods. Journal of Hydrology, 522, 339-352. https://doi.org/10.1016/j.jhydrol.2014.12.056

Vogelsang, C., Lusher, A. L., Dadkhah, M. E., Sundvor, I., Umar, M., Ranneklev, S. B., Eidsvoll, D., Meland, S. (2019). Microplastics in road dust–characteristics, pathways and measures. Norsk institutt for vannforskning. http://hdl.handle.net/11250/2493537

Wang, L., Wei, J., Huang, Y., Wang, G. Maqsood, I., (2011). Urban nonpoint source pollution buildup and washoff models for simulating storm runoff quality in the Los Angeles County. Environmental Pollution 159 (7), 1932–1940. https://doi.org/10.1016/j.envpol.2011.03.019

Wijesiri, B., Egodawatta, P., McGree, J., Goonetilleke, A., (2015a). Incorporating process variability into stormwater quality modelling. Sci. Total Environ. 533, 454–461. https://doi.org/10.1016/j.scitotenv.2015.07.008.

Wijesiri, B., Egodawatta, P., McGree, J., & Goonetilleke, A. (2015b). Process variability of pollutant build-up on urban road surfaces. Science of the Total Environment, 518, 434-440. https://doi.org/10.1016/j.scitotenv.2015.03.014

Zafra, C. A., Temprano, J., Tejero, I. (2008). Particle size distribution of accumulated sediments on an urban road in rainy weather. Environmental technology, 29(5), 571-582. https://doi.org/10.1080/09593330801983532.

Figure 1. Physical model scheme and initial distribution of the sediment.

Figure 2. Total suspended solids (TSS) and experimental flow results in both gully pots for the four different grain sizes (D1-D4) and rain intensities of 80, 50 and 30 mm/h. It can be seen that the complete pollutographs of the experiments have been a satisfactory measure here, through analyzing the manual grab samples for all the diameters and rain intensities.

Figure 3. TSS experimental results and five best-fitted TSS simulations for the experiments with rain intensities of 50 (up) and 80 mm/h (down) and sediment classes D2 and D3, respectively. It can be see that predictions agree well with experimental results. The contours of all the simulations performed in the global SA are also included (dashed lines), and illustrate the sensitivity of the model output to the plausible values of H-R parameters.

Figure 4. Standardized Regression Coefficients (SRC) of the Hairsine-Rose parameters for the total washed-off mass (row 1) and the TSS maximum value (row 2) in each gully pot (columns) and for each laboratory experiment (colours for the rain intensities and x-position for the sediment classes). The degree of transparency represents the R^2 value. The plots show that the critical mass is the most important H-R parameter and that there is a strong relation between the grain size of the sediment and the relative importance of rain-driven and flow-driven detachment parameters.

Figure 5. EFAST first order and total effect sensitivity indices of the Hairsine-Rose parameters for the total washed-off mass (row 1) and the TSS maximum value (row 2) in each gully pot (columns) and for each of the laboratory experiments (colors for rain intensities and x-position for sediment classes). It can be seen that the critical mass is the most important H-R parameter. α_0, h_0 and F occupy a secondary level of influence with respect to the total washed mass, but only F in the case of the TSS peak results.

Figure 6. Sensitivity results for the Elementary Effects method. Plots show the sensitivity to the total washed-off mass through gully pot 2 for each of the three rainfall intensities and four grain sizes considered in the experiments. The ranking of the three most influential input factors is shown in the upper-left corner of each case. In general, Ms_0, D_{50} and Ms_{cr} are the factors with the most influence on the result for all the laboratory experiments.

Figure 7. Sensitivity results for the Elementary Effects method. Plots show the sensitivity to the TSS maximum value in gully pot 2 in all cases. The ranking of the three most influential input factors is shown in the upper-left corner of each case. In general, Ms_0, D_{50}, Ms_{cr} and F are the factors with the most influence on results.

Table 1. Sediment granulometries considered (D1-D4) and total washed-off mass for the twelve laboratory experiments.

Sediment class	Granulometries				Washed-off mass (g)		
	D_{50} (µm)	D_{16} (µm)	D_{84} (µm)	σ_g	30 mm/h	50 mm/h	80 mm/h
D1	30.1	11.4	54.6	2.19	31.0	48.3	61.2
D2	68.1	46.3	91.8	1.41	13.2	32.5	53.8
D3	143.9	105.8	186.8	1.33	7.5	17.1	28.6
D4	273.8	204.7	351.8	1.31	6.1	13.6	22.9

Table 2. Parameters and ranges of variation used in the global sensitivity analysis.

Variable	Units	Definition	Range
α_0	$Kg/m^2/m$	Rainfall detachability coefficient	500 - 3500
h_0	M	Water depth damping threshold	0.0001 - 0.0025
b	-	Positive constant	0.6 - 1.4
Ms_{cr}	Kg/m^2	Critical mass to achieve the potential detachment	0 – 2.8
F	-	Effective fraction of excess stream power	0 - 0.03
Ω_0	W/m^2	Critical stream power	0 - 0.02

Table 3. Input factor ranges for the local sensitivity analysis.

Variable	R	n	IL	D_{50}	ρ_s	Ms_0	UC
Units	mm/h	-	Mm	μm	Kg/m^3	kg/m_{curb}	-
Uncertainty level	1	1	1	3	2	3	3
Range variation (%)	5	5	5	50	20	50	50
Lab. experiment							
1	29.25-30.75	0.0156-0.0164	0.585-0.615	22.5-37.5	2301-2812	15-25	0.24-0.40
2	48.75-51.25	0.0156-0.0164	0.585-0.615	22.5-37.5	2301-2812	15-25	0.24-0.40
3	78.00-82.00	0.0156-0.0164	0.585-0.615	22.5-37.5	2301-2812	15-25	0.24-0.40
4	29.25-30.75	0.0156-0.0164	0.585-0.615	51.0-85.0	2301-2812	15-25	0.24-0.40
5	48.75-51.25	0.0156-0.0164	0.585-0.615	51.0-85.0	2301-2812	15-25	0.24-0.40
6	78.00-82.00	0.0156-0.0164	0.585-0.615	51.0-85.0	2301-2812	15-25	0.24-0.40
7	29.25-30.75	0.0156-0.0164	0.585-0.615	108.0-180.0	2301-2812	15-25	0.24-0.40
8	48.75-51.25	0.0156-0.0164	0.585-0.615	108.0-180.0	2301-2812	15-25	0.24-0.40
9	78.00-82.00	0.0156-0.0164	0.585-0.615	108.0-180.0	2301-2812	15-25	0.24-0.40
10	29.25-30.75	0.0156-0.0164	0.585-0.615	205.5-342.5	2301-2812	15-25	0.24-0.40
11	48.75-51.25	0.0156-0.0164	0.585-0.615	205.5-342.5	2301-2812	15-25	0.24-0.40
12	78.00-82.00	0.0156-0.0164	0.585-0.615	205.5-342.5	2301-2812	15-25	0.24-0.40

Table 4. Ranges of Hairsine-Rose parameters for the local sensitivity analysis.

Variable	α_0	h_0	b	Ms_{cr}	F	Ω_0
Units	Kg/m^2/m	mm	-	Kg/m^2	-	W/m^2
Lab. experiment						
1	1504-3040	1.05-1.98	0.81-1.17	0.62-1.22	0.009-0.024	0.005-0.016
2	1614-2779	1.02-2.00	0.78-1.19	0.77-1.66	0.010-0.023	0.003-0.013
3	1589-2883	0.95-2.03	0.74-1.14	0.85-1.88	0.008-0.022	0.004-0.014
4	1536-2891	0.91-2.11	0.82-1.22	0.48-1.11	0.011-0.025	0.003-0.015
5	1557-2953	1.03-1.92	0.78-1.20	0.36-0.73	0.009-0.026	0.003-0.013
6	1364-2998	1.08-1.74	0.76-1.12	0.25-0.53	0.009-0.023	0.003-0.014
7	1391-2917	0.66-1.95	0.82-1.18	0.44-0.92	0.011-0.025	0.005-0.014
8	1602-2668	0.45-1.93	0.74-1.21	0.20-0.54	0.011-0.026	0.03-0.012
9	1647-2835	0.95-2.16	0.77-1.16	0.24-0.43	0.010-0.026	0.002-0.012
10	963-2556	0.72-2.11	0.88-1.21	0.25-0.59	0.013-0.026	0.004-0.013
11	1770-2629	0.89-1.96	0.83-1.30	0.14-0.31	0.009-0.025	0.004-0.015
12	1658-2755	1.19-2.07	0.85-1.21	0.12-0.22	0.010-0.025	0.005-0.014

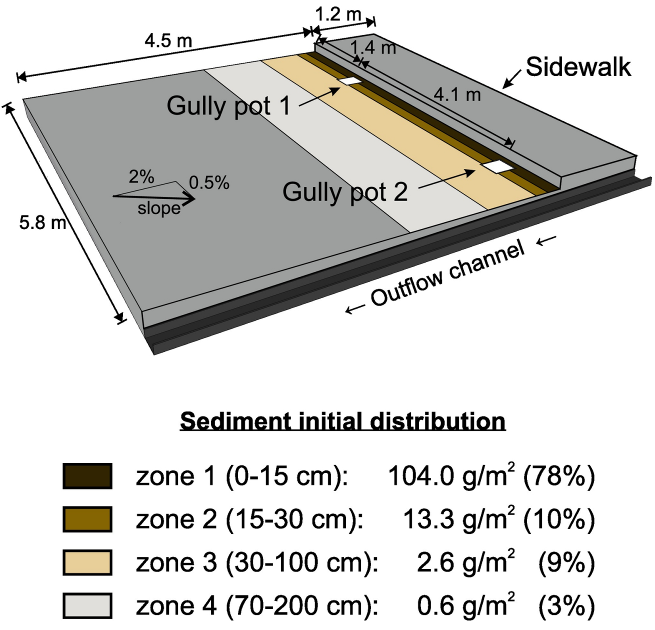
1.2 m
4.5 m
1.4 m
Sidewalk
4.1 m
Gully pot 1
2%
0.5%
slope
Gully pot 2
5.8 m
Outflow channel
Sediment initial distribution
zone 1 (0-15 cm): 104.0 g/m² (78%)
zone 2 (15-30 cm): 13.3 g/m² (10%)
zone 3 (30-100 cm): 2.6 g/m² (9%)
zone 4 (70-200 cm): 0.6 g/m² (3%)

Figure 1

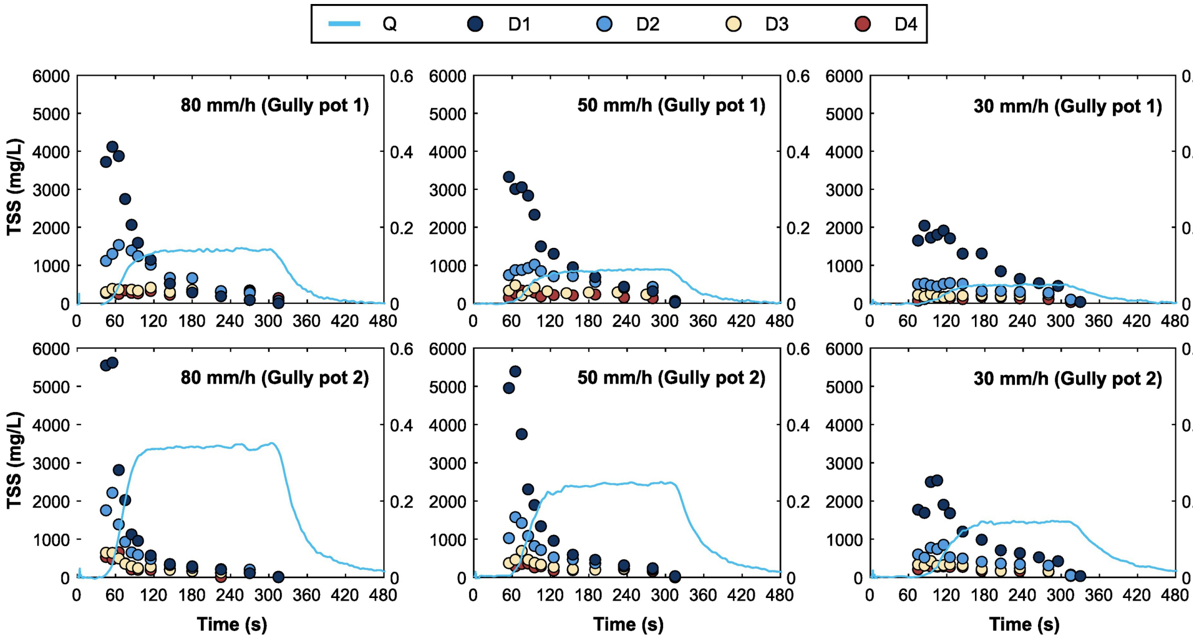
Q
D1
D2
D3
D4
80 mm/h (Gully pot 1)
50 mm/h (Gully pot 1)
30 mm/h (Gully pot 1)
80 mm/h (Gully pot 2)
50 mm/h (Gully pot 2)
30 mm/h (Gully pot 2)
TSS (mg/L)
Q (L/s)
Time (s)
0
60
120
180
240
300
360
420
480
1000
2000
3000
4000
5000
6000
0.2
0.4
0.6

Figure 2

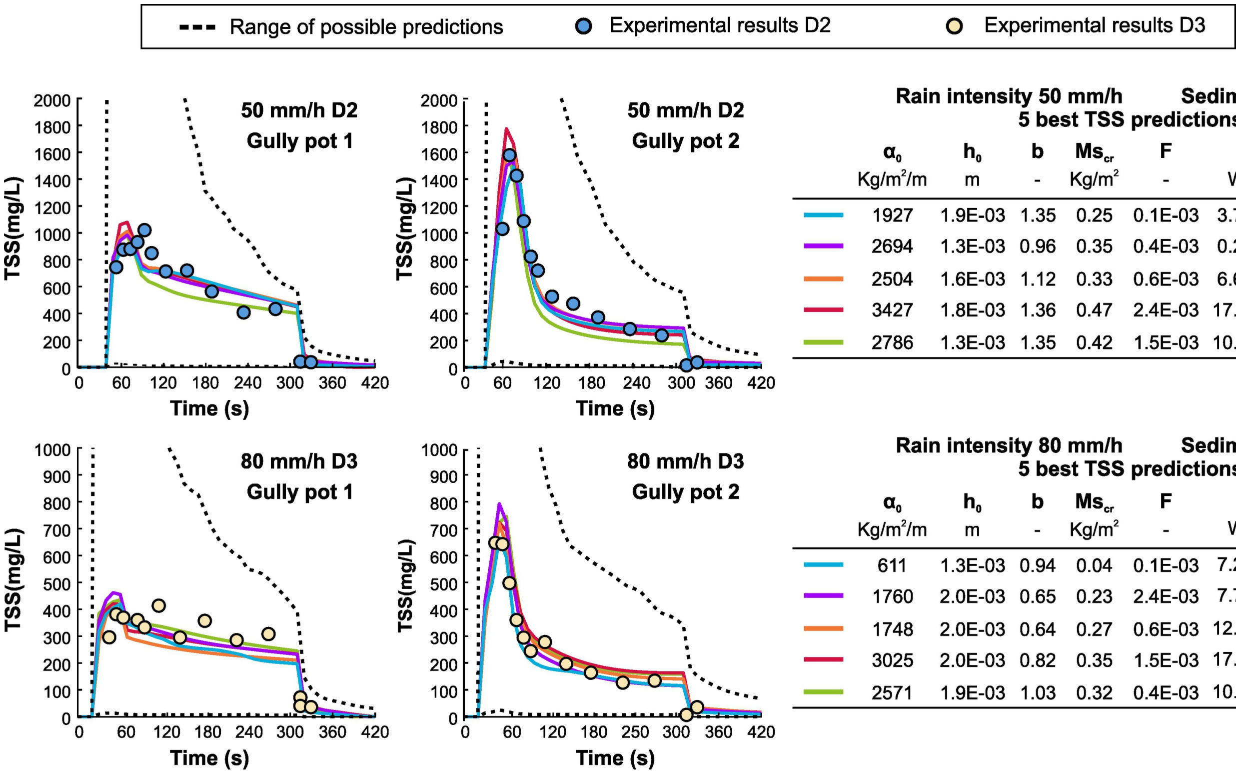

Rain intensity 50 mm/h **Sediment class D2**
5 best TSS predictions

α_0 Kg/m^2/m	h_0 m	b -	Ms_{cr} Kg/m^2	F -	Ω_0 W/m^2	NSE -
1927	1.9E-03	1.35	0.25	0.1E-03	3.7E-03	0.90
2694	1.3E-03	0.96	0.35	0.4E-03	0.2E-03	0.88
2504	1.6E-03	1.12	0.33	0.6E-03	6.6E-03	0.88
3427	1.8E-03	1.36	0.47	2.4E-03	17.8E-03	0.81
2786	1.3E-03	1.35	0.42	1.5E-03	10.5E-03	0.76

Rain intensity 80 mm/h **Sediment class D3**
5 best TSS predictions

α_0 Kg/m^2/m	h_0 m	b -	Ms_{cr} Kg/m^2	F -	Ω_0 W/m^2	NSE -
611	1.3E-03	0.94	0.04	0.1E-03	7.2E-03	0.84
1760	2.0E-03	0.65	0.23	2.4E-03	7.7E-03	0.81
1748	2.0E-03	0.64	0.27	0.6E-03	12.7E-03	0.81
3025	2.0E-03	0.82	0.35	1.5E-03	17.8E-03	0.80
2571	1.9E-03	1.03	0.32	0.4E-03	10.4E-03	0.79

Figure 3

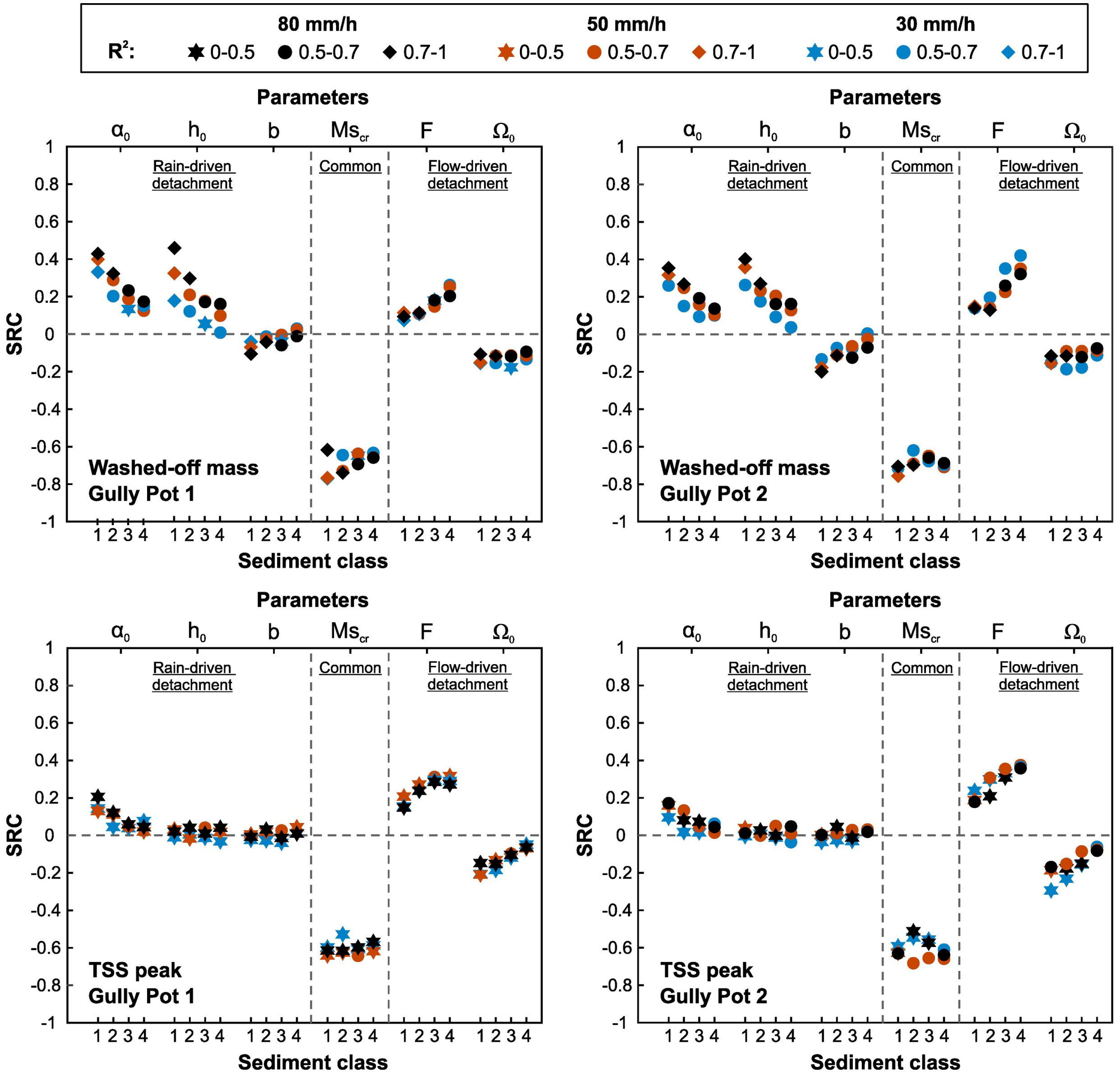
80 mm/h
50 mm/h
30 mm/h
R²:
0-0.5
0.5-0.7
0.7-1
Parameters
α₀
h₀
b
Ms_cr
F
Ω₀
Rain-driven detachment
Common
Flow-driven detachment
SRC
Sediment class
Washed-off mass Gully Pot 1
Washed-off mass Gully Pot 2
TSS peak Gully Pot 1
TSS peak Gully Pot 2

Figure 4

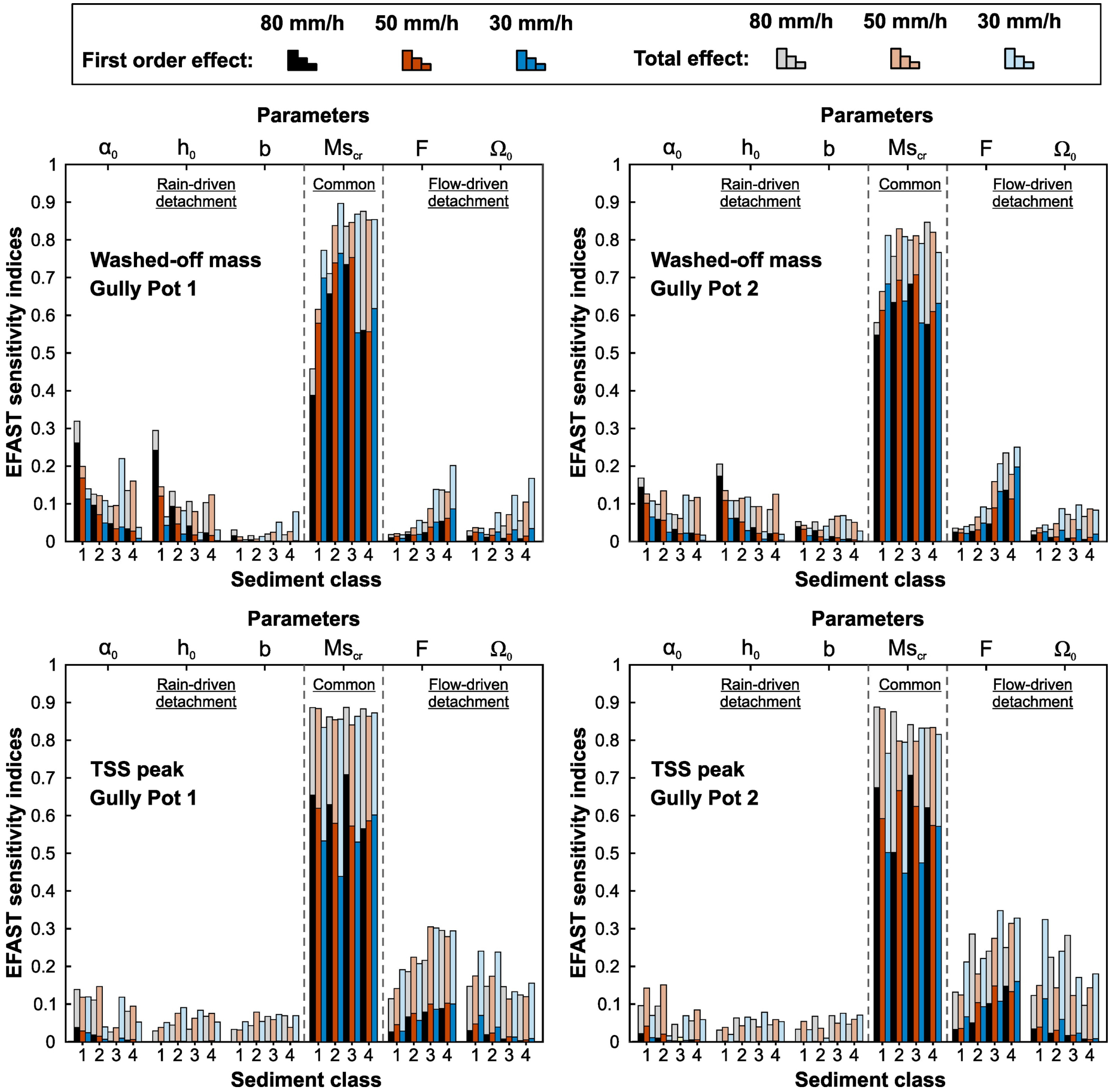
80 mm/h
50 mm/h
30 mm/h
First order effect:
Total effect:
Parameters
α0
h0
b
Mscr
F
Ω0
Rain-driven detachment
Common
Flow-driven detachment
EFAST sensitivity indices
Washed-off mass Gully Pot 1
Washed-off mass Gully Pot 2
TSS peak Gully Pot 1
TSS peak Gully Pot 2
Sediment class

Figure 5

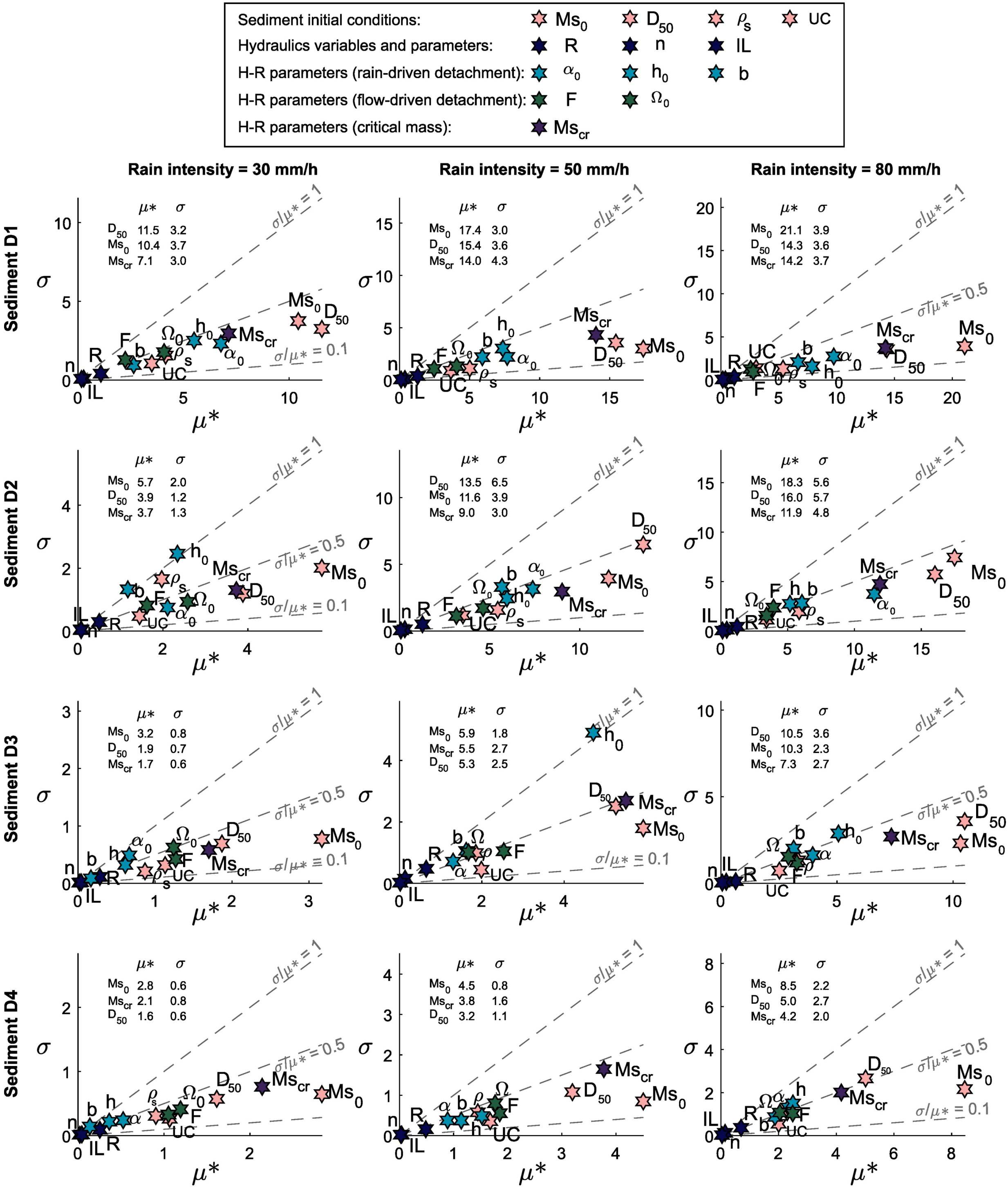

Sediment initial conditions:
Ms_0
D_{50}
ρ_s
UC
Hydraulics variables and parameters:
R
n
IL
H-R parameters (rain-driven detachment):
α_0
h_0
b
H-R parameters (flow-driven detachment):
F
Ω_0
H-R parameters (critical mass):
Ms_{cr}
Rain intensity = 30 mm/h
Rain intensity = 50 mm/h
Rain intensity = 80 mm/h
Sediment D1
Sediment D2
Sediment D3
Sediment D4
σ
$\mu*$
$\sigma/\mu* = 1$
$\sigma/\mu* = 0.5$
$\sigma/\mu* = 0.1$
$\mu*$ σ
D_{50} 11.5 3.2
Ms_0 10.4 3.7
Ms_{cr} 7.1 3.0
Ms_0 17.4 3.0
D_{50} 15.4 3.6
Ms_{cr} 14.0 4.3
Ms_0 21.1 3.9
D_{50} 14.3 3.6
Ms_{cr} 14.2 3.7
Ms_0 5.7 2.0
D_{50} 3.9 1.2
Ms_{cr} 3.7 1.3
D_{50} 13.5 6.5
Ms_0 11.6 3.9
Ms_{cr} 9.0 3.0
Ms_0 18.3 5.6
D_{50} 16.0 5.7
Ms_{cr} 11.9 4.8
Ms_0 3.2 0.8
D_{50} 1.9 0.7
Ms_{cr} 1.7 0.6
Ms_0 5.9 1.8
Ms_{cr} 5.5 2.7
D_{50} 5.3 2.5
D_{50} 10.5 3.6
Ms_0 10.3 2.3
Ms_{cr} 7.3 2.7
Ms_0 2.8 0.6
Ms_{cr} 2.1 0.8
D_{50} 1.6 0.6
Ms_0 4.5 0.8
Ms_{cr} 3.8 1.6
D_{50} 3.2 1.1
Ms_0 8.5 2.2
D_{50} 5.0 2.7
Ms_{cr} 4.2 2.0

Figure 6

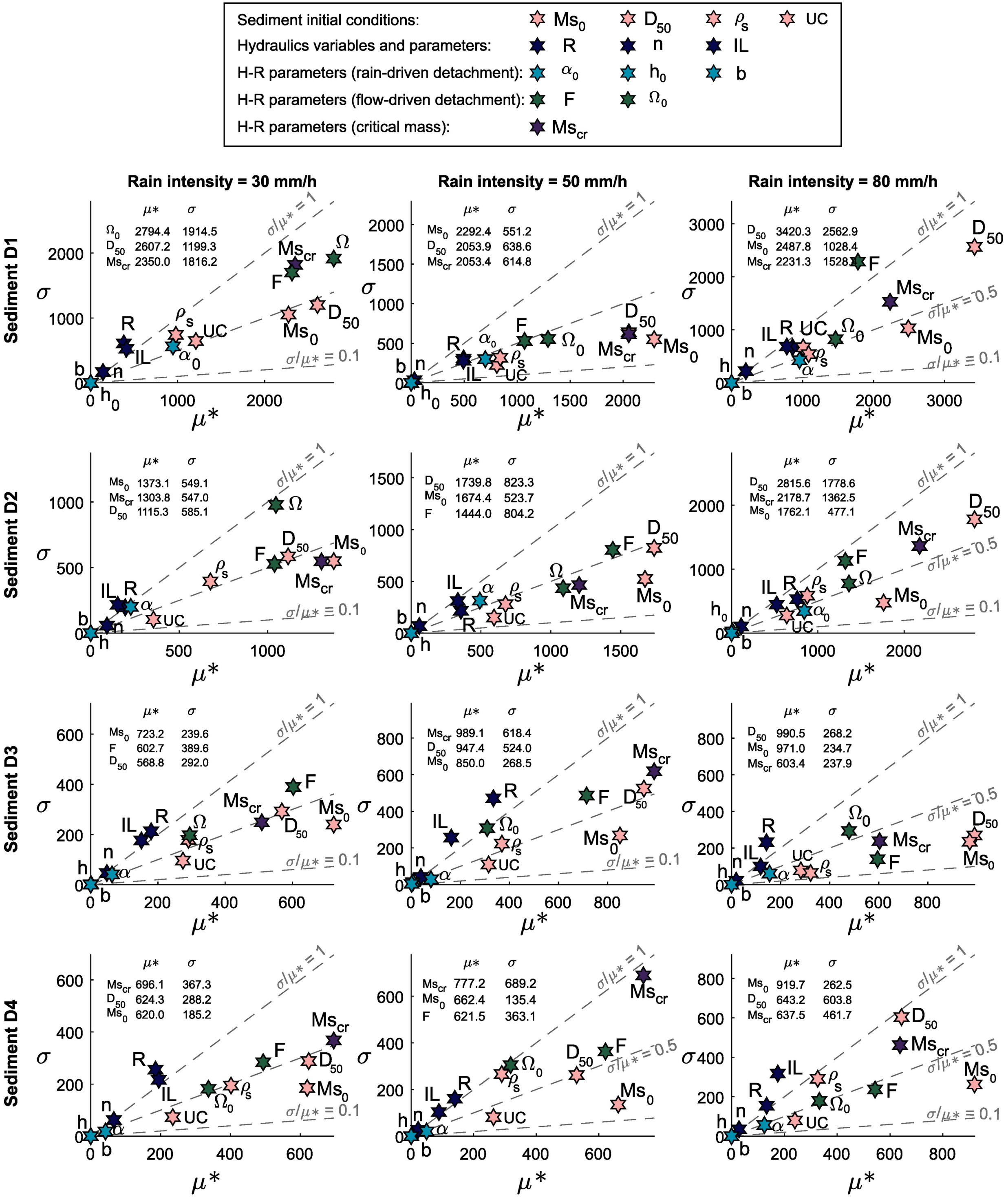

Figure 7